Electroexcitation of even-parity states in ^{27}Al

P. J. Ryan, R. S. Hicks, A. Hotta,* J. Dubach, G. A. Peterson, and D. V. Webb†
Department of Physics and Astronomy, University of Massachusetts, Amherst, Massachusetts 01003
(Received 20 December 1982)

Inelastic electron scattering form factors were measured for the even-parity states of ^{27}Al below 7 MeV. The data span a momentum transfer range of $q \simeq 0.57$–2.80 fm^{-1}. Separate longitudinal and transverse information was obtained, especially for the lowest-energy excitations. For excitations below 3.7 MeV, the longitudinal form factors were found to be well described by shell model calculations provided appropriate effective charges were introduced. These effective charges appear to exhibit little dependence on momentum transfer up to $q \simeq 2$ fm^{-1}. In contrast, effective charges or magnetic moments were not required to account for the corresponding transverse form factors. The shell model was somewhat less successful in its description of the higher-energy excitations, although tentative J^π assignments were made for some currently ambiguous states on the basis of a comparison with the theoretical predictions.

[NUCLEAR REACTIONS ^{27}Al(e,e'), $E=60$–340 MeV, $\theta=90°$, 160°, 180°; measured $\sigma(E,\theta)$, $\pi=+1$ levels, $E_x \leq 7$ MeV. Shell model theory.]

I. INTRODUCTION

The nucleus ^{27}Al has presented perhaps the greatest challenge to a comprehensive understanding of the $2s$-$1d$ shell. For example, the strong-coupling Nilsson-model description[1,2] is less satisfactory for ^{27}Al than it is for the deformed $A=21$–25 nuclei. More detailed interpretations have invoked appreciable band mixing,[3] the coupling of rotational and vibrational modes of motion,[4] or the strong interaction between particles in different Nilsson orbitals.[5] In contradiction to the prolate deformation indicated by the measured quadrupole moment,[6] Dehnhard[7] has even assumed an oblate shape to demonstrate that the strong-coupling model can account for both the enhanced $E2$ transition rates and the single-nucleon spectroscopic factors.

The weak-coupling model,[8–13] in which a proton hole is coupled to the collective rotational levels of ^{28}Si, also achieved some success in accounting for early measurements of electromagnetic transition rates and the inelastic scattering of light particles.[11,14,15] However, more precise measurements subsequently revealed serious deficiencies in the model, most particularly its inability[16–20] to predict the spectroscopic factors for single nucleon transfer. Indeed, application of the weak-coupling model is theoretically unsound[13] for the even-parity states of ^{27}Al since, from the microscopic viewpoint, the $d_{5/2}$ subshell into which the proton hole is coupled is already actively involved in the structure of the ^{28}Si states.

None of these models has been as successful in describing the even-parity levels of ^{27}Al as the large-basis shell-model calculations of Wildenthal and McGrory,[21] or Cole *et al.*[22] Comparison of the predicted and observed level spectra indicates that the structure of the low-lying even-parity states can be reasonably described in terms of the *sd*-shell configurations. This is further supported by evidence from stripping and pickup reactions. Moreover, these shell model calculations offer a consistent theoretical treatment of the mass region around ^{27}Al and avoid many of the inconsistencies in the various collective model approaches.

In this paper, we present electron scattering form factors for many of the even-parity states below 7 MeV. The availability of these comprehensive data provides a detailed test of the shell model calculations. Furthermore, if the model is found to reliably describe form factors for the excitation of well-known states, then the theoretical predictions might enable better definition of the spectroscopy of more poorly established levels. Most previous ^{27}Al(e,e') experiments[3,12,13,23–26] have lacked the fine resolution of the present measurement, and hence have failed to separate the more closely-spaced levels. In particular, little data have been previously reported for even-parity excitations above 3 MeV. This paper complements a previous publication[13] which

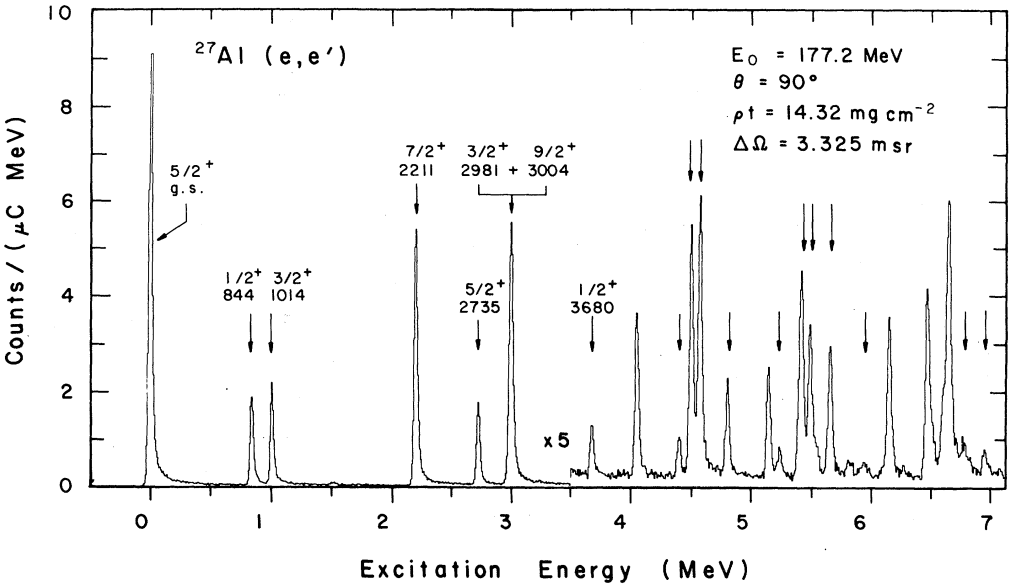

FIG. 1. Identification of even-parity states in a representative ^{27}Al(e,e') spectrum. The lower-energy peaks are labeled according to their excitation energies in keV. Obvious peaks not identified are known odd-parity states.

presented (e,e') data for the odd-parity states, and thus completes our study of the electroexcitation of ^{27}Al levels below 7 MeV.

II. EXPERIMENTAL DETAILS AND DATA ANALYSIS

The ^{27}Al(e,e') data presented in this paper were measured concurrently with those reported earlier[13] on the excitation of odd-parity states. For both sets of data the experimental procedures and data analysis techniques were identical, and thus only a few salient features are reported here.

The measurements were performed at the Bates Linear Accelerator Laboratory in Middleton, Massachusetts at scattering angles of 90°, 160°, and 180° for incident electron energies ranging from 60.3 to 339.1 MeV. The data span a momentum transfer range from 0.57 to 2.80 fm^{-1}. The targets consisted of high-purity aluminum foils of thickness 6.62 to 30.6 mg/cm^2.

A representative bin-sorted spectrum is displayed in Fig. 1. All established low-lying even-parity levels[27] were clearly seen except the weakly-excited 3.957 MeV level, and the 5.752 $(1/2)^+$ level. The resolution of this experiment, as fine as 26 keV full width at half maximum, permitted the peaks at 0.844 and 1.014 MeV to be readily separated, but was insufficient to differentiate the 2.981 and 3.004 MeV peaks. The latter were treated as an unresolved doublet in the analysis. Thus, the form factor measurements for most of the even-parity states below 7 MeV will be presented, although low-q data are sparse for the higher excited states. A complete tabulation of all data, including that for the odd-parity states, is available from the PAPS depository.[28]

III. THE SHELL MODEL

The $2s$-$1d$ shell model calculations discussed here assume that there is an inert core of eight neutrons and eight protons which provides no explicit contribution to the structure of the even-parity levels. The properties of these levels are then attributed solely to sd-shell nucleons. The calculations are thus performed by considering all possible sd-shell configurations allowed by the Pauli principle, although, to simplify the computation, model constraints have often been applied. For example, Van Hienen *et al.*[29] used a $d_{5/2}$ $s_{1/2}$ basis in which no nucleons were allowed to occupy the $d_{3/2}$ subshell. Wildenthal and McGrory[21] employed the full $d_{5/2}s_{1/2}d_{3/2}$ space, but constrained the number of $d_{5/2}$ nucleons to be greater than or equal to eight. Both calculations utilized a modified surface-delta (MSD) interaction with parameters chosen to reproduce selected features of the energy level spectrum.

The most extensive calculations that have been published are those of Cole *et al.*[22] These authors

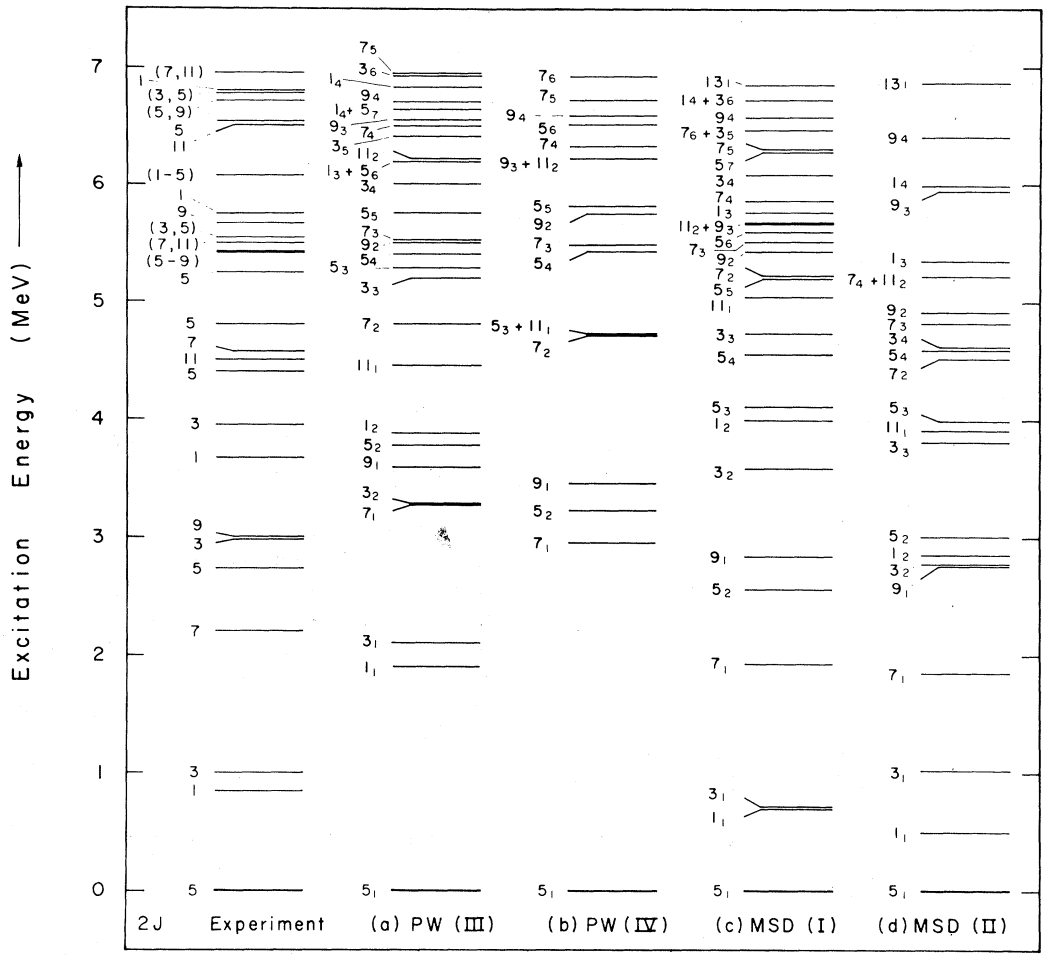

FIG. 2. Comparison of the observed even-parity spectrum of ^{27}Al with shell model results.

employed the Preedom-Wildenthal (PW) interaction[30] to perform calculations in the full $d_{5/2}s_{1/2}d_{3/2}$ space, as well as in a slightly truncated space where at least six nucleons were required to occupy the $d_{5/2}$ subshell. Because of the large size of these computations, the calculations in the untruncated *sd*-shell space were restricted to the $J^{\pi} \geq \frac{5}{2}^{+}$ levels. For the present analysis we have not only repeated all of the above shell model calculations, but have also examined the use of the Kuo-Brown[31] and Chung-Wildenthal[32] interactions. It was found that these latter interactions generally give results qualitatively similar to the PW interaction, and we will therefore restrict our discussion to the spaces and interactions summarized in Table I. The main emphasis will be placed on the results obtained with the PW interaction.

Figure 2 compares energy levels computed in these various models with the experimental ^{27}Al even-parity spectrum. Although precise agreement between the experimental and theoretical schemes is not achieved, it is clear that the shell model calculations are able to account for the high density of even-parity levels, whereas many of the collective

TABLE I. Model spaces and interactions discussed in the present work.

Notation	Configuration space	Truncation
PW(I)[a]	$d_{5/2}s_{1/2}$	$\langle d_{3/2} \rangle = 0$
PW(II)[a]	$d_{5/2}s_{1/2}d_{3/2}$	$\langle d_{5/2} \rangle \geq 8$
PW(III)[a]	$d_{5/2}s_{1/2}d_{3/2}$	$\langle d_{5/2} \rangle \geq 6$
PW(IV)[a]	$d_{5/2}s_{1/2}d_{3/2}$	none
MSD(I)[b]	$d_{5/2}s_{1/2}$	$\langle d_{3/2} \rangle = 0$
MSD(II)[c]	$d_{5/2}s_{1/2}d_{3/2}$	$\langle d_{5/2} \rangle \geq 8$

[a]Reference 30.
[b]Reference 29.
[c]Reference 21.

model approaches fail to do so. In any case, precise agreement between calculated and experimental energy levels is not as rigorous a test of the model as nuclear transition rates or electron scattering form factors.

The (e,e') form factors are related to the measured differential cross sections[33] by

$$\frac{d\sigma(k_i,\theta)}{d\Omega}=\left[\frac{Z\alpha\cos\theta/2}{2k_i\sin^2\theta/2}\right]^2\left[1+\frac{2k_i}{M}\sin^2\theta/2\right]^{-1}|F(q)|^2, \quad (1)$$

where $\vec{k}_i$ is the incident electron momentum, θ is the scattering angle, and M is the nuclear mass.

In the plane-wave Born approximation the form factor separates into longitudinal and transverse components, dependent only upon the three-momentum transfer q:

$$|F(q)|^2=|F_L(q)|^2+(\tfrac{1}{2}+\tan^2\theta/2)|F_T(q)|^2, \quad (2)$$

with

$$q^2=(\vec{k}_i-\vec{k}_f)^2$$

and $\vec{k}_f$ being the scattered electron momentum. Both the longitudinal and transverse form factors may be expressed as summations over the allowed multipole projections. With the assumption of an *sd*-shell space and one-body operators, $F_T(q)$ is restricted to the $M1$, $E2$, $M3$, $E4$, and $M5$ multipoles, whereas only $C0$, $C2$, and $C4$ may contribute to $F_L(q)$.

Since the present paper is primarily concerned with the ability of the shell model to describe general features, it was deemed adequate to calculate the form factors using simple single-particle harmonic oscillator wave functions. A value of $b=1.82$ fm was adopted[13] for the oscillator size parameter. For the range of momentum transfers investigated in this experiment, form factor calculations performed using more realistic wave functions derived from a Woods-Saxon potential well showed only minor differences in comparison to the harmonic oscillator results.

Since the shell model assumes that the nucleons are point particles inside a fixed potential well, two corrections must be applied before the theoretical form factors can be compared with data. In order to include the nucleon size, the form factors were multiplied by[33]

$$F_{SN}(q)=(1+q^2/18.744\ \text{fm}^{-2})^2 .$$

The lack of translational invariance of the shell model wave functions was accounted for by the center-of-mass correction factor

$$F_{\text{c.m.}}(q)=\exp(q^2b^2/4A) .$$

An additional correction is necessitated by the Coulomb distortion of the incident and scattered electron waves. Since the present data were obtained at many different incident electron energies, comparison with theory would normally be tedious because each electron energy requires a separate distorted wave calculation. However, for the present level of interpretation, and for the relatively low-Z nucleus ^{27}Al, tests showed that these small distortion effects can be sufficiently approximated by transforming the data to "effective" momentum transfers, given by[34]

$$q_{\text{eff}}=q(1+3Z\alpha/2k_iR) ,$$

where R represents the uniform-density charge radius, 3.94 fm for ^{27}Al (Ref. 35).

IV. RESULTS AND DISCUSSION

For states up to the (2.981-3.004) MeV unresolved doublet, sufficient data were taken both at 90° and at backward scattering angles to enable Rosenbluth separation of the longitudinal and transverse components of the form factors. However, the increasing level density at higher excitation energies hindered clear identification of the high-lying peaks in the poorer-resolution 160° and 180° spectra. Thus, although some transverse information was obtained on these excitations, most of the form factors for levels above 3.1 MeV were derived from the better-resolved 90° spectra. The resulting form factors are shown in Figs. 3–9, where the indicated error bars include statistical and some line-shape fitting uncertainties.

In what follows, we begin with a discussion of the longitudinal form factors for levels below 3.1 MeV, using these to establish the reliability of our model calculations. We then turn to the total form factors $|F(q)|^2$ of the higher-lying states which are generally predicted to be dominated by the longitudinal multipoles. These form factors provide further tests for the models. For states of unknown or ambigu-

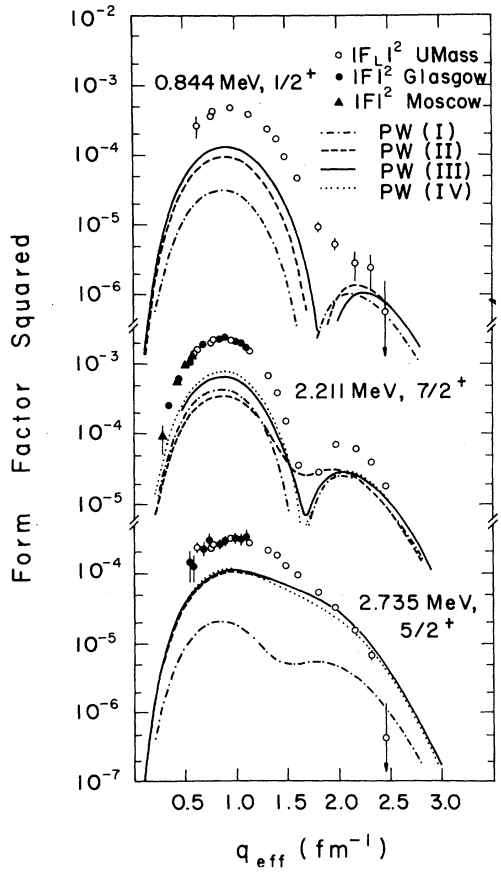

FIG. 3. Longitudinal form factors for three low-lying states in ^{27}Al, and comparison with various shell model calculations. Data from Glasgow (Ref. 12) and Moscow (Ref. 26) are included. The theoretical calculations shown here utilize bare nucleon charges.

ous spin-parity assignments, the data are compared with the model predictions with the hope of suggesting more definite assignments. Finally, the transverse form factors of the lowest-lying states are examined.

A. Longitudinal form factors for excitations below 3.1 MeV

A preliminary investigation was made of the dependence of the theoretical longitudinal form factors on the size of the shell-model configuration space. Figure 3 shows the results for excitations to the states at 0.844 MeV $(1/2)^+$, 2.211 MeV $(7/2)^+$, and 2.735 MeV $(5/2)^+$. The depicted data points include measurements made mainly at forward scattering angles by the Glasgow[12] and Moscow[26] groups.

The calculated $C2$ form factor for the $1/2^+$, 0.844 MeV level changes considerably as the model space is expanded. In particular, the magnitude increases by an overall factor of 2 to 3 in changing from the PW(I) basis to the PW(II) basis, and increases further, by a factor of 1.5, for PW(III). Clearly there are strong $d_{5/2} \leftrightarrow d_{3/2}$ $C2$ contributions which are not allowed in the $d_{5/2}s_{1/2}$ space. Similar effects may also be observed for the $7/2^+$, 2.211 MeV state and the $5/2^+$, 2.735 MeV state, although the form factor computed for the $7/2^+$ level actually decreases in the vicinity of $q \simeq 0.8$ fm^{-1} when the $d_{3/2}$ subshell is first included. However, the most striking feature of the calculations is their inability to reproduce the magnitude of the experimental form factors. Although the shapes are predicted satisfactorily, the theoretical curves obtained in the largest space still underestimate the data by a factor of 3 to 4.

These calculations explicitly assume that the core remains inert and that only the role of *sd*-shell nucleons need be considered. However, because of the polarizing effect of the extra-core nucleons, it is unrealistic to suppose the core plays no role. Using perturbation theory, Brussaard,[36] Horikawa *et al.*,[37] and others have demonstrated that excitations of nucleons from the $1s$ and $1p$ core orbitals and from the $2s$-$1d$ shell into higher shells contribute significantly to the electromagnetic transition rates. Thus, the shell model basis should be expanded even beyond the full $2s$-$1d$ space considered here, but this is not yet computationally feasible.

The effect of the truncation of the model is commonly parametrized by the introduction of isoscalar effective charges[38] (bare nucleon plus polarization charge) for the active nucleons. For example, instead of using bare values for the $2s$-$1d$ shell neutron and proton charges, Brown *et al.*[39,40] found empirically that respective values of $(e_p+e_n)=1.7e$ and $(e_p+e_n)\simeq 2e$ gave good agreement with $B(E2)$ and $B(E4)$ transition rates for many *sd*-shell transitions. These authors set the isovector charge (e_p-e_n) to the bare nucleon value of $1.0e$, since the isovector contributions to low-energy $E2$ and $E4$ transitions are generally small.

Examination of Fig. 3 shows that the effective charge value required to bring the theory into agreement with experiment depends very strongly on the particular configuration space being used. For example, a much larger value of (e_p+e_n) would be required for the $d_{5/2}s_{1/2}$ basis than for the spaces which include the $d_{3/2}$ subshell. However, the restriction to a single configuration space permits the study of the systematics of effective charge for a range of excitations. Since $J^\pi < 5/2^+$ levels were not computed in the largest model space [PW(IV)], we have utilized the next larger space, PW(III), for

TABLE II. Effective charges deduced from measured $B(E2\uparrow)$ values and $C2$ and $C4$ form factors.

J^π, E_{ex} (MeV)	$B(E2\uparrow)$[a] (e^2fm^4)	$(e_p+e_n)/e$ $E2$ ($q\simeq\omega$)	$(e_p+e_n)/e$ $C2$ (max)	$(e_p+e_n)/e$ $C4$
$1/2^+$, 0.844	12.7±0.5	1.70±0.03	1.85±0.05	
$3/2^+$, 1.014	25.5±2.6	1.93±0.10	1.92±0.04	
$7/2^+$, 2.211	94.6±5.4	2.10±0.06	1.97±0.09	1.39±0.32
$5/2^+$, 2.735	8±3[b]	1.52±0.26	1.62±0.05	1.07±0.02
$3/2^+$, 2.981				1.39±0.06[c]
$9/2^+$, 3.004	55.9±3.2	2.01±0.05	1.97±0.05	
$1/2^+$, 3.680	1.0±0.4[d]	1.88±0.32[d]	1.92±0.04	
$3/2^+$, 3.957			1.8 ±0.3	1.0 ±0.2
$11/2^+$, 4.510				1.74±0.06
$7/2^+$, 4.580				1.34±0.13

[a]Reference 27.
[b]Reference 13.
[c]Combining the $C4$ contributions of the 2.981 and 3.004 MeV states.
[d]Reference 41.

purposes of comparison. Two sets of isoscalar $C2$ effective charges (e_p+e_n) were obtained, one set from the $E2$ radiative transition rates at $q=\omega$, and the other set from the maxima of the $C2$ form factors. Similarly, by normalizing the theoretical $C4$ form factors to fit the data in the vicinity of the $C2$ diffraction minima, $C4$ effective charges were also deduced. In each case the isovector charge (e_p-e_n) was set equal to $1.0e$. These values, derived for many of the low-lying levels, are listed in Table II.

The average value deduced by comparison with measured $E2$ decay rates is

$$(e_p+e_n)=(1.86\pm0.14)e\ ,$$

identical to the average value deduced from the first maximum of the $C2$ form factor, $(1.86\pm0.09)e$. This contradicts claims by Radhi *et al.*[42] that the effective charges required to normalize the shell model calculations to the data are strongly q dependent at these momentum transfers. The average value of (e_p+e_n) for the $C4$ transitions was found to be $(1.3\pm0.1)e$, smaller than the value of $(2.0\pm0.2)e$ derived by Brown *et al.*[40] from $E4$ γ-ray decay rates observed in various *sd*-shell nuclei. The present value is closer to $1.15e$ as calculated by Horikawa *et al.*[37] using a microscopic core polarization model. Unfortunately, there currently exist no published $E4$ radiative transition rates for ground-state transitions in ^{27}Al, so that, in this low-q region, the q dependence of the $C4$ effective charge cannot be reliably studied.

These deduced average values for the $C2$ and $C4$ isoscalar effective charges were then employed in our calculations of the remaining ^{27}Al form factors. For the $C0$ multipole, which contributes to the electroexcitation of $5/2^+$ states, no effective charge was used; since there are far fewer possible configurations that can contribute, the $C0$ effective charge may be expected to be closer to $1.0e$.

Figure 4 shows the results of these calculations for those excitations where complete longitudinal-transverse separations were possible. The theoretical form factor for the unresolved 3.0 MeV doublet was obtained by adding the form factors predicted for the $3/2_2^+$ and $9/2_1^+$ states. Although the theoretical curve overestimates the high-q data for the $5/2^+$, 2.735 MeV level, there exists general agreement between theory and experiment. Thus, provided appropriate effective charges are adopted, the shell model calculations give a reasonable description of the longitudinal form factors for these low-lying even-parity ^{27}Al levels, at least for momentum transfers up to $q\simeq1.5$ fm^{-1}. At higher momentum transfers, the theoretical curves tend to overestimate the data, implying that smaller effective charge values are required. The assumption of q-independent effective charges therefore seems to be limited to the region below 2 fm^{-1}, in accordance with the theoretical predictions of Horikawa *et al.*[43] and Horsfjord[44] for ^{15}N and the oxygen isotopes. With this caution in mind, all shell model calculations presented henceforth utilize constant $C2$ and $C4$ isoscalar effective charges equal to $1.86e$ and $1.30e$.

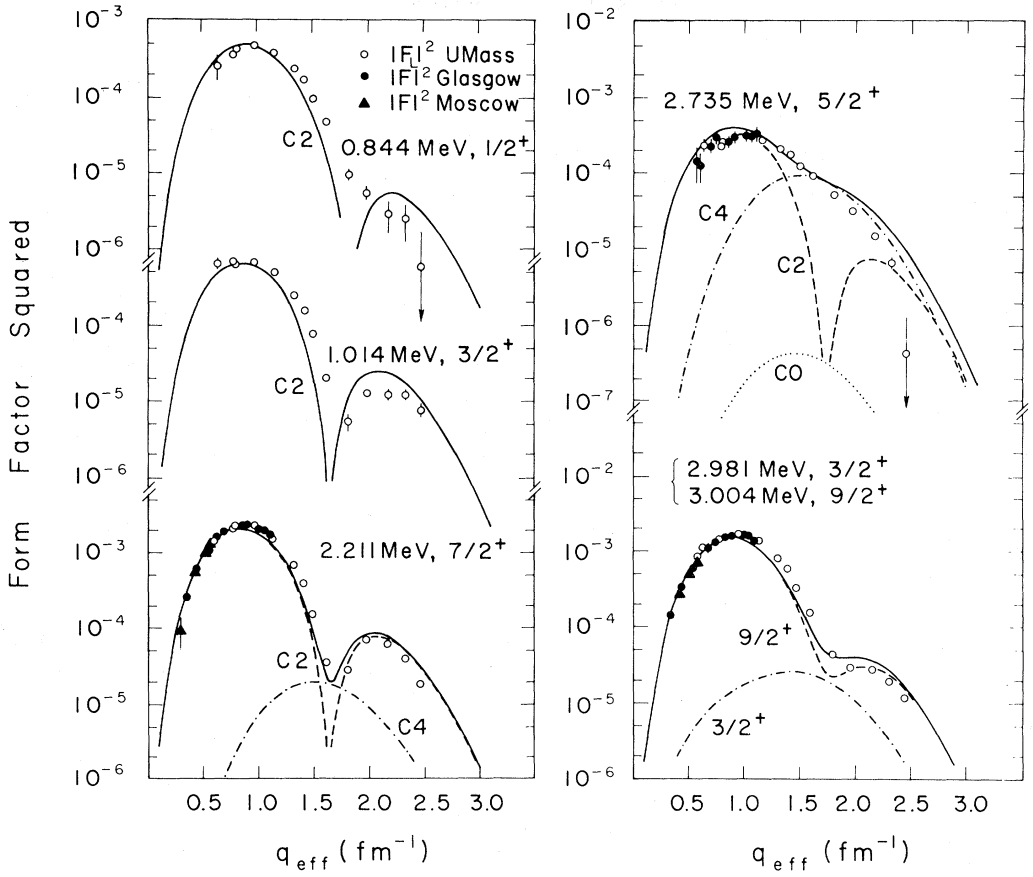

FIG. 4. Longitudinal form factors for low-energy excitations in ^{27}Al, and comparison with PW(III) shell model calculations employing empirically-derived isoscalar effective charges (e_p+e_n) for the $C2$ and $C4$ multipole operators. In the case of the unresolved 3.0 MeV doublet, the continuous curve represents the summed form factors of the predicted $3/2_2^+$ and $9/2_1^+$ levels.

B. Higher-lying states

Encouraged by the good agreement between theory and experiment for the lowest excited states, we extend our critique of the shell model to even-parity states above 3.1 MeV. Recent ^{26}Mg$(p,\gamma)^{27}$Al measurements by Maas *et al.*[45] and Smit *et al.*[46] have considerably clarified the spin and parity assignments in this region. Nevertheless, the spins of some levels observed here, such as the 5.500 MeV state, have not yet been established. As previously mentioned, a secondary objective of the present investigation was to utilize the comparison with the shell model predictions to suggest firmer assignments for some of the unknown or ambiguous states.

The total form factors for the higher-lying levels were deduced mainly from the 90° spectra and often, although not always, appear to be dominated by longitudinal components. The results for the levels at 3.680 MeV $(1/2)^+$, 3.957 MeV $(3/2)^+$, 4.510 MeV $(11/2)^+$, and 4.580 MeV $(7/2)^+$ are plotted in Fig. 5. Comparisons are made with the predicted total form factors $|F|^2$, which have been decomposed to show the longitudinal $|F_L|^2$ and transverse $1.5|F_T|^2$ contributions at $\theta=90°$. Correspondence between the observed and shell-model levels was made solely on the basis of the J^π assignment and excitation energy.

Except for the $3/2^+$ 3.957 MeV state, the predicted form factors are predominantly longitudinal. For this level, the calculated transverse form factor dominates the total form factor at low-q values; however, it also overestimates the limited transverse data available. For the other three levels the few transverse data points, $1.5|F_T|^2$, are in better quantitative agreement with the theoretical calculations.

Of particular interest is the form factor for the

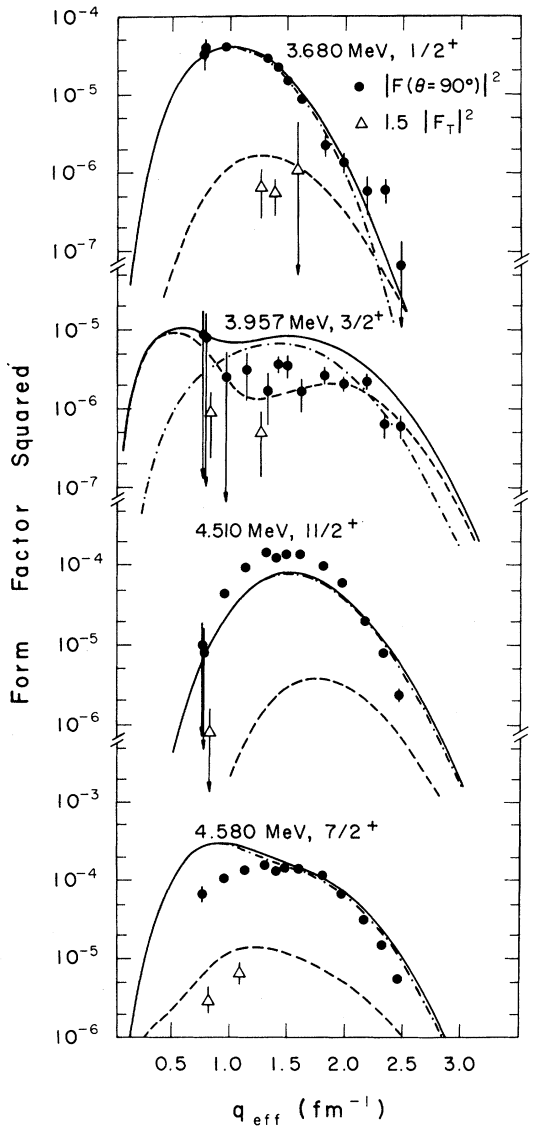

FIG. 5. Form factors for four excitations in the 3.6–4.6 MeV region. The total theoretical form factor at 90° (continuous curve) is equal to the sum of the longitudinal (dashed-dotted) and transverse (dashed) curves. Note that both the transverse data and the transverse curves have been multiplied by 1.5 to include the kinematic factor $(1/2+\tan^2\theta/2)$ evaluated at 90°.

electroexcitation of the $11/2^+$ state at 4.510 MeV. The assumption of a pure *sd*-shell space not only restricts the form factor to the *C*4 multipole, but also permits only *d*-shell orbits to contribute. Since the form factor shape can therefore be expected to be relatively model independent, it is noteworthy that the calculated curve decreases too slowly at high q. Although the predicted shape could be somewhat improved by a 10% increase in the *d*-orbit size parameter, we attribute the discrepancy to the core-polarization effects implicated by the need for an effective charge. As was found for the *C*2 isoscalar effective charge, the *C*4 effective charge appears to decrease rapidly above 2 fm^{-1}. For the model spaces investigated here, isoscalar effective charges of less than 1.0*e* seem to be required above $q \simeq 2.0$ fm^{-1}. Inspection of other form factors with strong *C*4 contributions shows the same result: At high q the predicted form factors exceed the data.

In general, agreement between theory and experiment is slightly worse for the levels shown in Fig. 5 than for the lower-lying excited states. A possible explanation for the deterioration of the model lies in the inadequacy of the phenomenological parametrization of the nucleon-nucleon interaction. This inadequacy will be emphasized in regions densely populated by states having the same isospin and J^π assignments. For example, the lowest observed $J^\pi = 1/2^+$ levels are located at 0.844, 3.680, and 5.752 MeV and may be readily associated with the levels predicted at 1.907, 3.904, and 6.192 MeV in the PW(III) spectrum. Since these levels are well separated in energy, there is little possibility of strong mixing or of making a false assignment for a given level. Thus, not surprisingly, the shell model calculations provide good agreement with the data for the lowest $1/2^+$ levels, as shown in Figs. 4 and 5.

In contrast, the density of observed and predicted $5/2^+$ levels is far higher. In addition to the ground, 2.735, and 4.410 MeV states, the recent spectroscopic work[45,46] has revealed definite $5/2^+$ levels at 4.812 and 5.248 MeV, with the possibility of additional $5/2^+$ levels at 5.420, 5.433, and 5.551 MeV. Form factors for these levels are plotted in Fig. 6. The 5.420 and 5.433 MeV levels lie unresolved with a definite $5/2^-$ state[46] at 5.438 MeV. The data for the 4.410, 4.812, and 5.248 MeV levels are seen to lie in poor agreement with the form factors corresponding to the third, fourth, and fifth levels predicted by the PW(III) shell model calculation. In particular, the shell model substantially underestimates the $q \leq 1$ fm^{-1} data on the latter three excitations. For the case of the 4.410 MeV excitation, the available transverse data indicate that the principal deficiency of the theory lies in the prediction of the low-q transverse strength. The character of the unaccounted strength therefore suggests the presence of a strong *M*1 component not given by the theory. Mixing-ratio data[27] also support the existence of appreciable *M*1 strength in this transition. It is noteworthy that the 4.410 MeV data seem to be more consistent with the theoretical form factor for

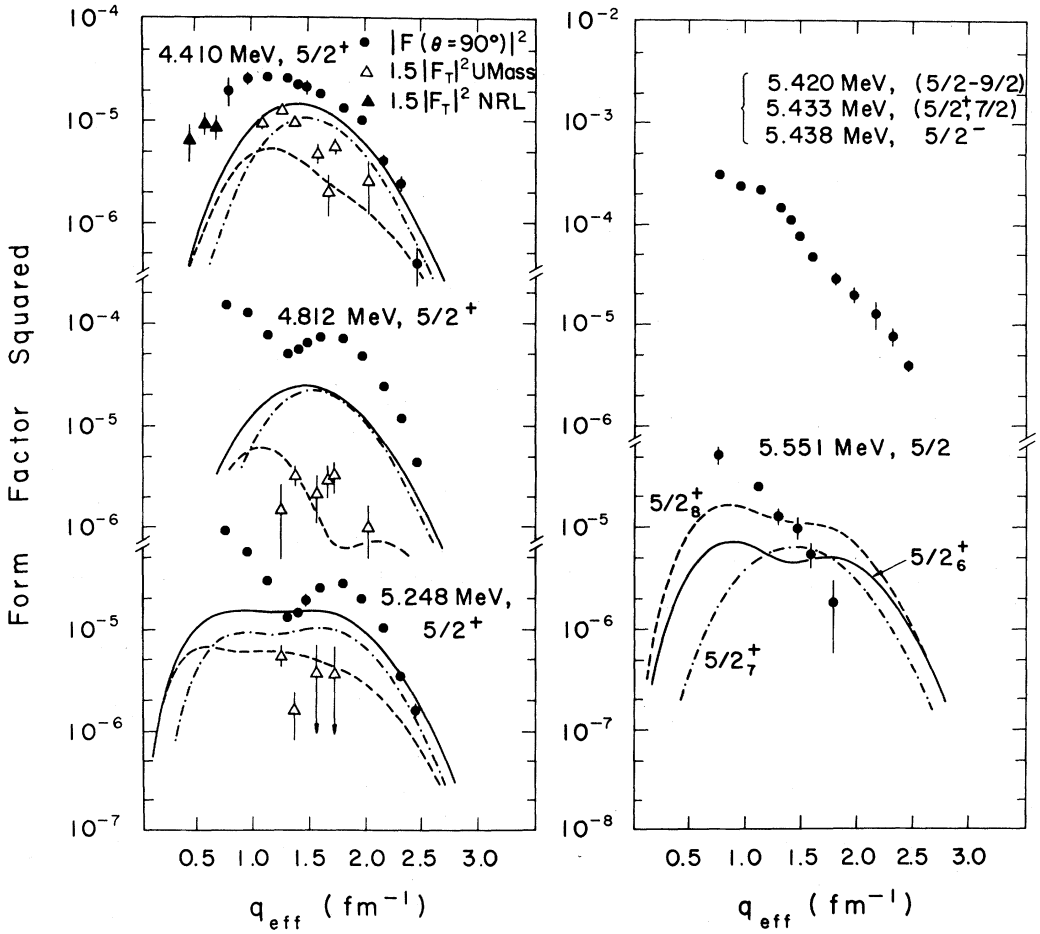

FIG. 6. Form factors for definite and possible $5/2^+$ levels in ^{27}Al. For the established $5/2^+$ states at 4.410, 4.812, and 5.248 MeV, the theoretical longitudinal and transverse components are displayed according to the conventions used in Fig. 5. The three curves compared to the 5.551 MeV data belong to the sixth, seventh, and eighth predicted $5/2^+$ states.

the fifth $5/2^+$ level, which is shown in comparison with data on the 5.248 MeV excitation.

Inspection of the low-q 180° spectra measured by Fagg *et al.*[25] shows that the transverse strength in the 4.812 and 5.248 MeV excitations is less than 50% of that for the 4.410 MeV level. Thus the 90° transverse contribution to the 4.812 and 5.248 MeV form factors will be less than 5×10^{-6}, whereas the observed low-q data are of order 10^{-4}. Moreover, the higher-q transverse data are reasonably described by the theoretical prediction. These observations suggest that, in these two cases, it is the longitudinal form factors, not the transverse, that are incorrectly described by the model. Poorly-predicted $C2$ multipoles may account for these discrepancies. For example, the $C2$ form factor of the fourth predicted $5/2^+$ level, shown in comparison with the 4.812 MeV data, has a q dependence markedly different from the characteristic $C2$ shapes shown in Figs. 3 and 4. In this case the model gives a $C2$ form factor which peaks at a momentum transfer more typical of that expected for a $C4$ transition. On the other hand, the $C2$ form factor of the fifth predicted $5/2^+$ level, compared to the 5.248 MeV data, has the desired shape, but is at least an order of magnitude smaller than would be required to account for the low-q measurements. Even if the ordering is altered and the theoretical counterparts for these $5/2^+$ levels have been incorrectly assigned, the large low-q cross sections measured for the 4.812 and 5.248 MeV transitions cannot be explained: The shell model appears to misrepresent the configuration admixture in the closely-spaced $5/2^+$ states.

As can be seen from Figs. 4 and 6, the shape of

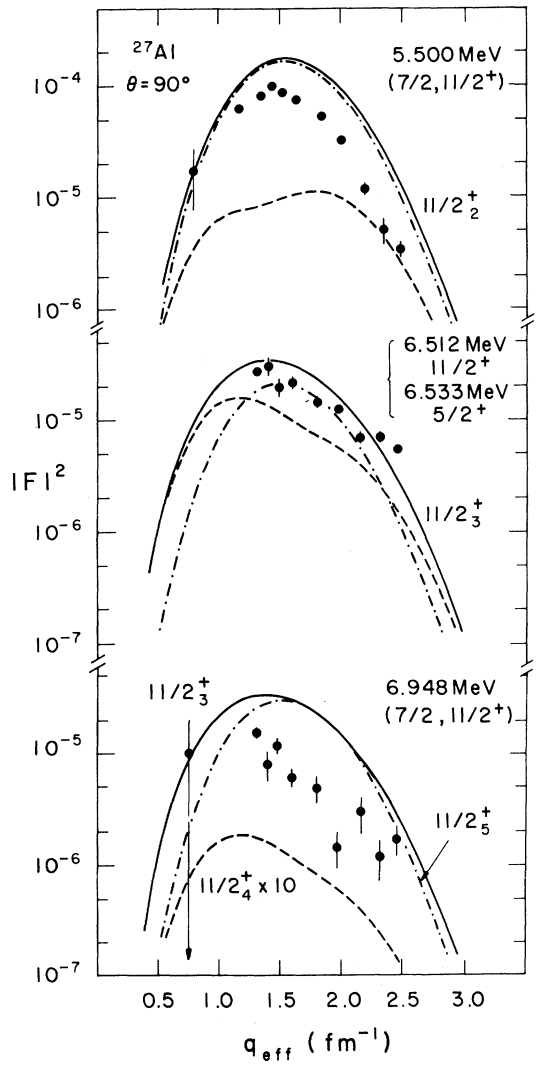

FIG. 7. Form factors determined at $\theta=90°$ for excitations appearing to have strong $C4$ multipoles. The theoretical curves for the 5.500 MeV peak and 6.52 MeV doublet are drawn according to the conventions used in Fig. 5. The three curves compared to the 6.948 MeV data belong to the third, fourth, and fifth predicted $11/2^+$ levels.

the form factor measured for the 5.551 MeV 5/2 state is unlike that observed for any resolved $5/2^+$ state. Nor do any of the theoretical form factors for predicted $5/2^+$ states bear any resemblance to the data. Although a $5/2^-$ assignment may therefore be suspected, the measured q dependence is not readily reconcilable with that observed by Hicks *et al.*[13] for odd-parity states.

Of the form factors remaining to be discussed, Fig. 7 shows those that appear to be dominated by $C4$ multipole contributions. The level at 5.500 MeV is restricted to assignments[27] of 7/2 or $11/2^+$; however, the shape of its form factor closely resembles that of the $11/2^+$, 4.510 MeV state, suggesting that it is the second $11/2^+$ level in the ^{27}Al spectrum. Moreover, the gamma-ray branching-ratio data[27] also lend weight to an $11/2^+$ assignment rather than $7/2^+$ or $7/2^-$. This level decays principally (79%) to the $9/2^+$, 3.004 MeV state with a smaller branch (21%) to the $7/2^+$, 2.211 MeV state. If the assignment is $11/2^+$, the decay to the $9/2^+$ level should occur mainly via an $M1$ transition while the decay to the $7/2^+$ level should be mainly $E2$ which, *a priori*, would be expected to be weaker. On the other hand, an assignment of $7/2^-$ would result in both γ decays being of $E1$ character, while a $7/2^+$ assignment would lead to both decays being of $M1$ character. Thus, while hardly conclusive, the branching-ratio data support the $11/2^+$ assignment, in accordance with the electron scattering data. The theoretical curve for the $11/2_2^+$ level is plotted in Fig. 7 and qualitatively agrees with the data in the same way as was observed for the first $11/2^+$ state, shown in Fig. 5.

Figure 7 also shows the form factor for the 6.52 MeV unresolved doublet containing the $5/2^+$, 6.512 MeV and $11/2^+$, 6.533 MeV levels.[27] The form factor calculated for the third $11/2^+$ level shows qualitative agreement with the data, suggesting that it is the $11/2^+$ member which provides the dominant contribution.

The level at 6.948 MeV is assigned as $(7/2,11/2^+)$. None of the form factors computed for candidate $7/2^+$ levels bears any resemblance to the data, so that this level is either strongly mixed with neighboring $7/2^+$ levels, belongs to the odd-parity spectrum, or has an assignment of $11/2^+$. As was the case for the 5.500 MeV level, the γ-decay data seem to favor an $11/2^+$ assignment with a strong $M1$ branch (67%) to the $9/2^+$, 3.004 MeV state and a weaker $E2$ branch (24%) to the $7/2^+$, 2.211 MeV state. For purposes of comparison, form factors calculated for the third, fourth, and fifth $11/2^+$ levels are included in Fig. 7.

Finally, Fig. 8 shows the 90° form factors measured for the levels at 5.668, 5.960, and 6.713 MeV. The theoretical form factor for the second $9/2^+$ state lies in good agreement with the 5.668 MeV data, especially considering the high excitation energy. The 5.960 MeV levels has spin 7/2, but unknown parity. The PW(III) calculation predicts $7/2^+$ levels at 5.53, 6.50, 6.95, and 7.45 MeV. Although the computed $7/2_5^+$ form factor shows some similarity to the data, the data are also comparable to the form factor shape observed by Hicks *et al.*[13]

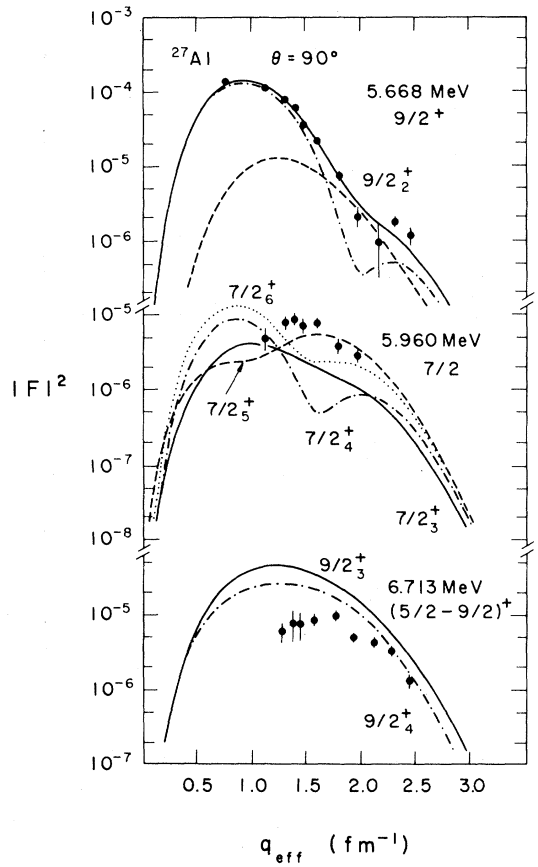

FIG. 8. Form factors for the 5.668, 5.960, and 6.713 MeV excitations. The longitudinal and transverse components of the theoretical predictions for the 5.668 MeV excitation are plotted according to the conventions of Fig. 5. Data for the 5.960 MeV level of undetermined parity are compared to form factors calculated for the third to sixth predicted $7/2^+$ levels. In the case of the 6.713 MeV form factor, the curves belong to the third and fourth predicted $9/2^+$ levels.

for a $C3$, $1p \rightarrow 1d$ transition. Hence, the parity assignment of this level is still not clear.

The spin and parity of the 6.713 MeV level is currently restricted[27] to $5/2^+$, $7/2^+$, or $9/2^+$. However, none of the form factors for $5/2^+$ or $7/2^+$ candidate theoretical levels bears any resemblance to the data. As shown in Fig. 8, the calculated form factors for the third and fourth $9/2^+$ levels, which have strong $C4$ multipole contributions, exhibit qualitative similarity to the shape of the experimental form factor, although they considerably overestimate its magnitude.

C. Transverse form factors

We now proceed to the discussion of the transverse form factors deduced for the even-parity levels below 3.1 MeV. Transverse form factors for the states at 0.844 MeV $(1/2)^+$, 1.014 MeV $(3/2)^+$, 2.211 MeV $(7/2)^+$, and 2.735 MeV $(5/2)^+$ were computed in the different configuration spaces using bare-nucleon values for both the charges and magnetic moments. The results are plotted in Fig. 9. As was the case for the longitudinal form factors, there is a general tendency for the agreement between theory and experiment to improve as the basis space is enlarged. Contrasting with the longitudinal calculations, however, is the lack of any pronounced and systematic trend accompanying the progression to the larger spaces.

On the average, the magnitudes of the measured transverse form factors lie in reasonable agreement with the values obtained in the largest calculated model spaces. Thus, given the statistical precision of the measurements reported here, and the fact that the transverse form factors for these levels usually consist of many overlapped electric and magnetic multipoles, it is not at all clear whether effective charges and g factors are necessary to describe the transverse data. In any case, such effective charges and g factors would be required to be small. Brown *et al.*[39] have calculated effective g factors for the $M3$ and $M5$ operators in *sd*-shell nuclei using a zero-range interaction between the core and valence particles. The results they obtained do not substantially differ from the bare nucleon values. For both $M3$ and $M5$ transitions, reductions of less than 25% and 8% are predicted for the proton and neutron g factors, respectively. These are certainly not inconsistent with the present findings. Little gamma-ray data exist for $M3$ and $M5$ transitions, so that the predictions of Ref. 39 cannot be checked directly at the photon point.

It appears, therefore, that, unlike the longitudinal form factors, the transverse form factors show little sensitivity to contributions involving single-particle orbits outside the *sd*-shell. Examination of the composition of the transition density matrices reveals that, whereas the isovector components undergo little change as the *sd*-shell model space is expanded, the isoscalar components tend to increase. A possible explanation for this phenomenon lies with the isospin dependence of the nucleon-nucleon interaction which lowers the energy of isoscalar transition strength with respect to isovector strength. Thus, as the model space is increased, proportionately more isoscalar strength is mixed into the low-lying excitations. Neglecting convection current terms, the ratio of isovector to isoscalar contributions for trans-

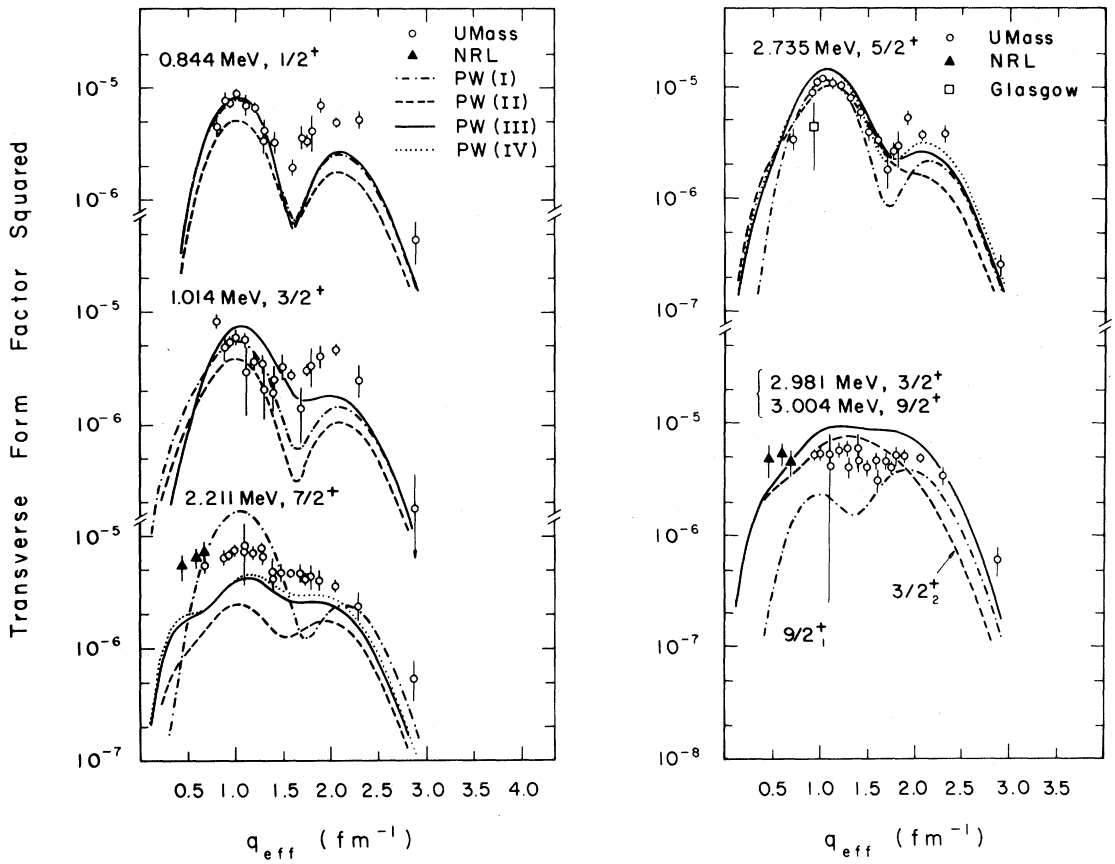

FIG. 9. Transverse form factors for low-lying states in ^{27}Al. The 0.844, 1.014, 2.211, and 2.735 MeV measurements are compared to shell model calculations utilizing the PW interaction in four different model spaces. In the case of the unresolved 3.0 MeV doublet, the continuous curve represents the summed contributions of the PW(III) form factors calculated for the $9/2_1^+$ (dotted-dashed) and $3/2_2^+$ (dashed) levels.

verse excitation is of the order

$$(\mu_p-\mu_n)^2/(\mu_p+\mu_n)^2\sim 28\ ,$$

so that the computed transverse form factor is rather insensitive to the isoscalar contribution, particularly at high q. On the other hand, for longitudinal excitation the isovector to isoscalar ratio is proportional to

$$(e_p-e_n)^2/(e_p+e_n)^2\ ,$$

equal to 1.0 for bare charge values. Consequently, the longitudinal form factor will be appreciably affected by an increased isoscalar contribution. A continuation of this trend, namely, that as the model space is expanded beyond the *sd*-shell, substantial increases are realized in the isoscalar density matrix elements along with relatively minor modifications to the isovector elements, could provide a simultaneous explanation for both the longitudinal and the transverse form factors.

Finally, the shape of the transverse form factor for the 3.0 MeV doublet, also shown in Fig. 9, is reasonably well described. At lower momentum transfers it is the 2.981 MeV form factor that is predicted to provide the main transverse contribution, in direct contrast to the overwhelming dominance of the 3.004 MeV excitation in the longitudinal form factor. This is in good agreement with mixing-ratio data,[27] which indicate that the radiative width of the 2.981 MeV state to the ground state is dominated by the $M1$ contribution, with the $E2$ contribution being insignificant ($<1\%$).

V. SUMMARY AND CONCLUSIONS

Shell model calculations have been extensively tested by comparison with electroexcitation data on the even-parity levels of ^{27}Al. For the longitudinal form factors, it was demonstrated that bare charge values lead to theoretical predictions that are far smaller than the data. Effective charges for the *sd*-shell nucleons were therefore introduced to parametrize effects not explicitly included in the model; for example, excitations from the 1*p*-core orbits and from the 2*s*-1*d* shell to higher shells. By comparing the experimental data with the theoretical calculations, low-q isoscalar effective charge values (e_p+e_n) of $(1.86\pm0.1)e$ and $(1.3\pm0.1)e$ were determined for the $C2$ and $C4$ multipole operators. With the inclusion of these parameters, the longitudinal form factors of the relatively isolated, low-lying states ($E_x \leq 3.680$ MeV) are well described up to about $q=2$ fm^{-1}, whereupon the required effective charges begin to decrease.

The application of this procedure to higher-lying excitations met with mixed success. For example, the form factors predicted for the three established $5/2^+$ levels at 4.410, 4.812, and 5.248 MeV provide only a crude description of the data, suggesting that the theoretical calculations do not correctly mix these closely-spaced levels. In other cases, however, tentative J^π assignments could be proposed for currently ambiguous levels.

Whereas effective charges were required to describe the longitudinal form factors of the lowest-lying excited states, adequate agreement between theory and experiment for the corresponding transverse form factors was achieved using bare values for charges and magnetic moments. Transverse electroexcitation of these low-lying ^{27}Al levels is apparently determined mainly by the 2*s*-1*d* shell nucleons, with relatively little contribution from other shells.

Of the stable *sd*-shell nuclei, ^{27}Al is recognized as being one of the most computationally difficult to model. The present investigation has shown, however, that the low-lying even-parity states are reasonably well described by current *sd*-shell model calculations. In common with all other shell model calculations, one of the least satisfying aspects of the theory is the necessity of introducing large and *ad hoc* effective charges to account for the observed magnitude of the $C2$ and $C4$ form factors. Since this is known to be a direct consequence of the truncation of the shell model space, a more complete investigation of the role of other shells is of obvious merit. The separate determination of both the longitudinal and transverse form factors as presented here should provide valuable checks of the consistency of such studies.

ACKNOWLEDGMENTS

We are indebted to our colleagues who assisted with the data taking during the long course of this experiment. This work was financially supported by the U.S. Department of Energy and the Japanese Ministry of Education.

---

*Permanent address: Department of Liberal Arts, School of Physics, Shizuoka University, Shizuoka 422, Japan.

†Permanent address: Australian Radiation Laboratory, Yallambie, Victoria 3085, Australia.

[1]K. H. Bhatt, Nucl. Phys. 39, 375 (1962).

[2]G. R. Bishop, Nucl. Phys. 14, 376 (1960).

[3]C. L. Lin and F. J. Kline, Proceedings of Sendai Conference on Electro- and Photo-excitations, Sendai, Japan, 1977, Tohoku University Laboratory of Nuclear Science Research Report, Vol. 10, Supplement, 1977 (unpublished).

[4]H. Ropke, V. Glattes, and G. Hammel, Nucl. Phys. A156, 477 (1970).

[5]H. G. Price, P. J. Twin, A. N. James, and J. F. Sharpey-Schafer, J. Phys. A 7, 1151 (1974).

[6]R. Weber, B. Jeckelmann, J. Kern, U. Kiebele, B. Aas, W. Beer, I. Beltrami, K. Bos, G. De Chambrier, P. F. A. Goudsmit, H. J. Leisi, W. Ruckstuhl, G. Strassner, and A. Vacchi, Nucl. Phys. A377, 361 (1982).

[7]D. Dehnhard, Phys. Lett. 38B, 389 (1972).

[8]V. K. Thankappan, Phys. Rev. 141, 957 (1966).

[9]D. Evers, J. Hertel, T. W. Retz-Schmidt, and S. J. Skorka, Nucl. Phys. A91, 472 (1967).

[10]R. M. Lombard and G. R. Bishop, Nucl. Phys. A101, 625 (1967).

[11]G. M. Crawley and G. T. Garvey, Phys. Lett. 19, 228 (1965); Phys. Rev. 167, 1070 (1968).

[12]R. P. Singhal, A. Johnston, W. A. Gillespie, and E. W. Lees, Nucl. Phys. A279, 29 (1977).

[13]R. S. Hicks, A. Hotta, J. B. Flanz, and H. de Vries, Phys. Rev. C 21, 2177 (1980).

[14]H. Niewodniczanski, J. Nurzynski, A. Strzalkowski, J. Wilczynski, J. R. Rook, and P. E. Hodgson, Nucl. Phys. 55, 386 (1964).

[15]J. Kokame, K. Fukunaga, and H. Nakamura, Phys. Lett. 14, 234 (1964).

[16]W. P. Alford, D. Cline, H. E. Gove, K. H. Purser, and S. Skorka, Nucl. Phys. A130, 119 (1969).

[17]W. Bohne, H. Fuchs, K. Grabisch, M. Hagen, H. Homeyer, U. Janetzki, H. Lettau, K. H. Maier, H. Morgenstern, P. Pietrzyk, G. Roschert, and J. A. Scheer, Nucl. Phys. A131, 273 (1969).

[18]H. E. Gove, K. H. Purser, J. J. Schwartz, W. P. Alford, and D. Cline, Nucl. Phys. A116, 369 (1968).

[19]B. H. Wildenthal and E. Newman, Phys. Rev. 167, 1027 (1968).

[20]H. Mackh, G. Mairle, and G. J. Wagner, Z. Phys. 269, 353 (1974).

[21]B. H. Wildenthal and J. B. McGrory, Phys. Rev. C 7, 714 (1973).

[22]B. J. Cole, A. Watt, and R. R. Whitehead, J. Phys. G 1, 935 (1975).

[23]R. M. Lombard and G. R. Bishop, Nucl. Phys. A101, 601 (1967).

[24]T. Terasawa, K. Nakahara, M. Oyamada, H. Saito, and E. Tanaka, Tohoku University Laboratory of Nuclear Science Research Report, 1972 (unpublished), Vol. 4, p. 27.

[25]L. W. Fagg, W. L. Bendel, R. A. Lindgren, and E. C. Jones, Phys. Rev. C 16, 923 (1977).

[26]B. S. Dolinskii, R. L. Kondratev, N. N. Kostin, V. P. Lisin, V. N. Ponomarev, and A. L. Polonskii, Izv. Akad. Nauk SSSR, Ser. Fiz. 45, 188 (1981). [Bull. Acad. Sci. USSR, Phys. Ser. 45, 166 (1981)].

[27]P. M. Endt and C. van der Leun, Nucl. Phys. A310, 1 (1978).

[28]See AIP document No. PAPS PRVCA-27-2515-18 for 18 pages of tabulated cross section measurements. Order by PAPS number and journal reference from American Institute of Physics, Physics Auxiliary Publication Service, 335 East 45th Street, New York, NY 10017. The price is $1.50 for microfiche or $5 for photocopies. Airmail additional. Make checks payable to the American Institute of Physics.

[29]J. F. A. Van Hienen, P. W. M. Glaudemans, and J. Van Lidth de Jeude, Nucl. Phys. A225, 119 (1974).

[30]B. M. Preedom and B. H. Wildenthal, Phys. Rev. C 6, 1633 (1972).

[31]T. T. S. Kuo, Nucl. Phys. A103, 71 (1967).

[32]W. Chung, Ph.D. thesis, Michigan State University, 1976 (unpublished).

[33]T. de Forest and J. D. Walecka, Adv. Phys. 15, 1 (1966).

[34]D. G. Ravenhall and D. R. Yennie, Proc. Phys. Soc. London A70, 857 (1957).

[35]C. W. deJager, H. deVries, and C. deVries, At. Data Nucl. Data Tables 14, 479 (1974).

[36]P. J. Brussaard, Nukleonika 19, 481 (1974).

[37]Y. Horikawa, T. Hoshino, and A. Arima, Phys. Lett. 63B, 134 (1976).

[38]B. H. Wildenthal, Nukleonika 23, 459 (1978).

[39]B. A. Brown, W. Chung, and B. H. Wildenthal, Phys. Rev. C 21, 2600 (1980).

[40]B. A. Brown, W. Chung, and B. H. Wildenthal, Phys. Rev. C 22, 774 (1980).

[41]A. Anttila, M. Bister, A. Luukkainen, A. Z. Kiss, and E. Somorjai, Nucl. Phys. A385, 194 (1982).

[42]R. Radhi, W. Chung, B. A. Brown, and B. H. Wildenthal, Bull. Am. Phys. Soc. 27, 574 (1982).

[43]Y. Horikawa, T. Hoshino, and A. Arima, Nucl. Phys. A278, 297 (1977).

[44]V. Horsfjord, Nucl. Phys. A253, 216 (1975).

[45]J. W. Maas, A. J. C. D. Holvast, A. Baghus, H. J. M. Aarts, and P. M. Endt, Nucl. Phys. A301, 237 (1978).

[46]J. J. A. Smit, J. P. L. Reineke, M. A. Meyer, D. Reitmann, and P. M. Endt, Nucl. Phys. A377, 15 (1982).